

Temperature trends of the permittivity in complex oxides of rare-earth elements with perovskite-type structure

A.G.Belous, O.V.Ovchar, D.O.Mischuk

V.I.Vernadskii Institute of General and Inorganic Chemistry
32/34 Palladina Ave., 03680 Kyiv 142, Ukraine

Received September 4, 2002

Ceramic materials based on complex oxides with both the perovskite structure ($\text{Ln}_{2/3}\text{Nb}_2\text{O}_6$) and the structure of tetragonal tungsten bronze ($\text{Ba}_{6-x}\text{Ln}_{8+2x/3}\text{Ti}_{18}\text{O}_{54}$) have been investigated over a wide frequency and temperature ranges. The results obtained for certain structures denote the presence of the temperature anomalies of dielectric parameters (ϵ , $\tan \delta$). These anomalies occur over the wide frequency range including submillimeter (SMM) wavelength range, and are related neither with the processing peculiarities nor with the presence of the phase transitions. Temperature behavior of the permittivity has been considered in terms of the polarization mechanism based on the elastic-strain lattice oscillations. It has been assumed that the observed anomalies could be ascribed to a superposition of harmonic and anharmonic contribution to lattice oscillations that determines τ_ϵ sign and magnitude.

Key words: dielectric permittivity, dielectric loss, microwave dielectrics

PACS: 77.22.-d, 77.22.Ch

1. Introduction

The growing demand for the microwave (MW) products induces the a need of new ceramic materials that combine a high relative permittivity ($\epsilon \gg 1$), low dielectric loss ($\tan \delta < 10^{-3}$) and a low temperature coefficient of permittivity ($\tau_\epsilon = \pm 1-100$ ppm/K). These materials are urgently required to reduce the size and the weight of radio equipment. Recently, very promising temperature stable ceramic materials with high permittivity (of about 100) have been developed on the basis of the defect perovskite $\text{Ln}_{2/3}\text{TiO}_3$ (Ln is rare-earth element) [1,2]. This structure contains 1/3 vacant positions in the lanthanum sublattice that permits aliovalent substitution of the lanthanum ions by lower valence ions, for example, alkali and/or alkaline-earth ions. When vacant sites are filled with alkali ions M^+

– for instance, by sodium ions – according to the formula $\text{Ln}_{2/3-x}\text{M}_{3x}\text{TiO}_3$, high-permittivity dielectrics with the perovskite structure are formed [2].

When titanium ions in $\text{Ln}_{2/3}\text{TiO}_3$ are replaced by smaller niobium ions, a defect perovskite structure $\text{Ln}_{2/3}\text{Nb}_2\text{O}_6$ may be obtained [3,4]. This structure is similar to $\text{Ln}_{2/3}\text{TiO}_3$, and exhibits high permittivity in the medium frequency range ($\epsilon = 200$ when $\text{Ln} = \text{La}$). However, there are few experimental data related to MW dielectric properties of $\text{Ln}_{2/3}\text{Nb}_2\text{O}_6$ which only assume that complex niobates $\text{Ln}_{2/3}\text{Nb}_2\text{O}_6$ may have negative τ_ϵ in the vicinity of room temperature. Therefore, one could expect that partial structure stabilization by sodium ions in the system $(1 - 3x/2)\text{Ln}_{2/3}\text{Nb}_2\text{O}_6 - 3x\text{NaNbO}_3$ may result in the temperature compensation of the permittivity due to the positive sign of τ_ϵ of antiferroelectric NaNbO_3 close to room temperature. It is known that the perovskite structure of niobates $\text{Ln}_{2/3}\text{Nb}_2\text{O}_6$ could be also stabilized by either alkali or alkaline-earth ions [5,6]. However, complex barium niobates formed in the latter exhibit ferroelectricity and high dielectric loss at room temperature in the MW range [6] which forbids their utilization as MW dielectrics.

In the case when a defect perovskite $\text{Ln}_{2/3}\text{TiO}_3$ is stabilized by alkaline-earth ions, for instance barium ions, solid solutions $\text{Ba}_{6-x}\text{Ln}_{8+2x/3}\text{Ti}_{18}\text{O}_{54}$ (known as barium lanthanide titanates – BLTs) with the structure of tetragonal tungsten bronze are formed [7,8]. Both sign and magnitude of temperature coefficient τ_ϵ of the above materials strongly depend on chemical composition, particularly on the ionic radii of rare-earth elements [7–9]. Moreover, in the materials $\text{Ba}_{6-x}\text{Sm}_{8+2x/3}\text{Ti}_{18}\text{O}_{54}$, temperature anomalies of the dependencies of the dielectric parameters ($\epsilon, \tan \delta$) have been revealed, and have shown a direct effect on the temperature coefficient τ_ϵ [9]. However, physical backgrounds of the observed phenomena are still under discussion.

Therefore, the target of this work was to investigate dielectric properties (ϵ and $\tan \delta$) of the promising high- ϵ materials based on complex oxides $\text{Ln}_{2/3}\text{Nb}_2\text{O}_6$ ($\text{Ln} = \text{La}, \text{Nd}$) and $\text{Ba}_{6-x}\text{Ln}_{8+2x/3}\text{Ti}_{18}\text{O}_{54}$ ($\text{Ln} = \text{La}, \text{Nd}, \text{Sm}$) over the wide frequency and temperature ranges, and to discuss the nature of temperature stabilization of the permittivity.

2. Experiment

Polycrystalline samples, prepared by conventional ceramic technique, have been examined. Extra pure and reagent grade oxides and carbonates were used as starting reagents. The starting reagents were initially mixed and ball-milled in agate bowls in acetone during 4 hours. The mixed blend was then dried and the powders were calcined at 1000–1200 °C in the air, pressed, and sintered at 1300–1400 °C during 2 hours in the air. The phase composition and the lattice parameters of the materials were analyzed with x-ray powder diffraction (XRD) using a DRON 3 diffractometer and Cu K_α radiation. Temperature and frequency behavior of the permittivity (ϵ), and dielectric loss tangent ($\tan \delta$) were measured by means of Q-meters at the frequencies of 10^4 – 10^7 Hz, by means of coaxial line at the frequencies of about 10^9 Hz, and by a modified-dielectric-resonator method at the frequency of

10^{10} Hz. Submillimeter-wave (SMM) frequency measurements were carried out using a backward-wave tube, by measuring the optical-path length and the absorption (α) in a parallel-plate sample coated with a quarter-wavelength anti-reflecting coating.

3. Results

3.1. System $(1 - 3x/2)\text{Ln}_{2/3}\text{Nb}_2\text{O}_6 - 3x\text{NaNbO}_3$ (Ln = La, Nd)

The materials $\text{La}_{2/3}\text{Nb}_2\text{O}_6$ and $\text{Nd}_{2/3}\text{Nb}_2\text{O}_6$ are characterized by high permittivity of 130 and 160, respectively, and by relatively low dielectric loss in the MW range (in both cases $\tan \delta$ is of the order of $(2-5) \cdot 10^{-3}$). The results of measurements of electrophysical properties of complex niobates $\text{Ln}_{2/3}\text{Nb}_2\text{O}_6$ (Ln = La, Nd) over wide frequency (10^6-10^{10} Hz) and temperature (-100 °C – $+100$ °C) ranges denote the change in the trends of temperature dependencies of the permittivity $\epsilon(T)$ with increasing measurement frequency (figure 1). When the measurement frequency increases, τ_ϵ value close to the room temperature ($\tau_{\epsilon(20-100^\circ\text{C})}$), which is about of $+100$ ppm/K at 10^6 Hz, changes to -1000 ppm/K at 10^{10} Hz. Moreover, the diffuse anomalous regions have been revealed for the first time on the temperature dependencies of the permittivity of $\text{Ln}_{2/3}\text{Nb}_2\text{O}_6$ collected at 10^{10} Hz (figure 1a). It should be noted that the regions of the anomalies revealed are observed at low temperatures, and shift for about 30 °C towards higher temperatures when changing rare-earth element from La to Nd. Again, the anomalies of the permittivity are accompanied by the anomalies in the temperature dependencies of $\tan \delta(T)$ (figure 1b). Most likely, the nature of the anomalies observed is not related to the presence of spontaneously polarized state because the variation of $\epsilon(T)$ in the vicinity of the anomalies does not follow Curie-Weiss law.

According to the results of XRD analysis when introducing sodium ions into the sublattice of rare-earth element in the systems $(1 - 3x/2)\text{Ln}_{2/3}\text{Nb}_2\text{O}_6 - 3x\text{NaNbO}_3$ solid solutions with the perovskite structure are formed. When introducing sodium ions into sublattice of rare-earth element, the permittivity continuously increases at $0 \leq x \leq 1/2$, and reaches the values of 600 and 1000 at room temperature for the lanthanum and neodymium containing solid solutions, respectively at $x = 1/2$ (figure 2). In the case of $x > 1/2$, the permittivity decreases towards the values of about 200 (NaNbO_3). The dispersion of the permittivity has not been detected for all materials investigated within the frequency range of 10^6-10^{10} Hz. It should be noted that for all materials studied the magnitude of $\tan \delta$ continuously increases with the increasing measurement frequency, and reaches 10^{-1} at the frequency 10^{10} Hz which makes it impossible to use them at extra high frequencies (EHF). Measurement results denote the change in the sign of temperature coefficient τ_ϵ within the compositional range corresponding to $(1/3 \leq x \leq 1/2)$ in the case of La-containing materials, and $(1/2 \leq x \leq 7/12)$ in the case of Nd-containing analogues.

Both lanthanum and neodymium containing materials with the composition $(1 - 3x/2)\text{Ln}_{2/3}\text{Nb}_2\text{O}_6 - 3x\text{NaNbO}_3$ at $x \geq 1/2$ have phase transitions above room temperature which shift towards higher temperatures with the increase of sodium

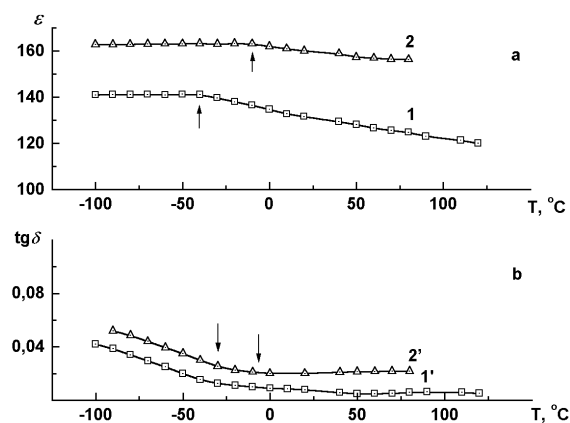


Figure 1. Temperature dependencies of the permittivity (1, 2) and dielectric loss tangent (1', 2') of the materials $\text{Ln}_{2/3}\text{Nb}_2\text{O}_6$ (1, 1' – Ln = La; 2, 2' – Ln = Nd) measured at 10^{10} Hz.

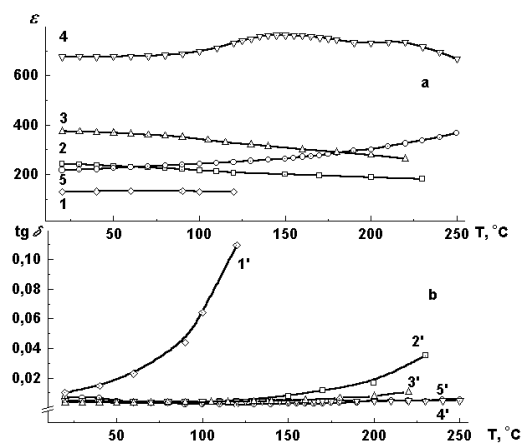


Figure 2. Temperature dependencies of the permittivity (1–5) and dielectric loss tangent (1' – 5') of the materials $(1 - 3x/2)\text{Ln}_{2/3}\text{Nb}_2\text{O}_6 - 3x\text{NaNbO}_3$; $x = 0$ (1); 1/6 (2); 1/3 (3); 1/2 (4); 2/3 (5) – measured at 10^6 Hz.

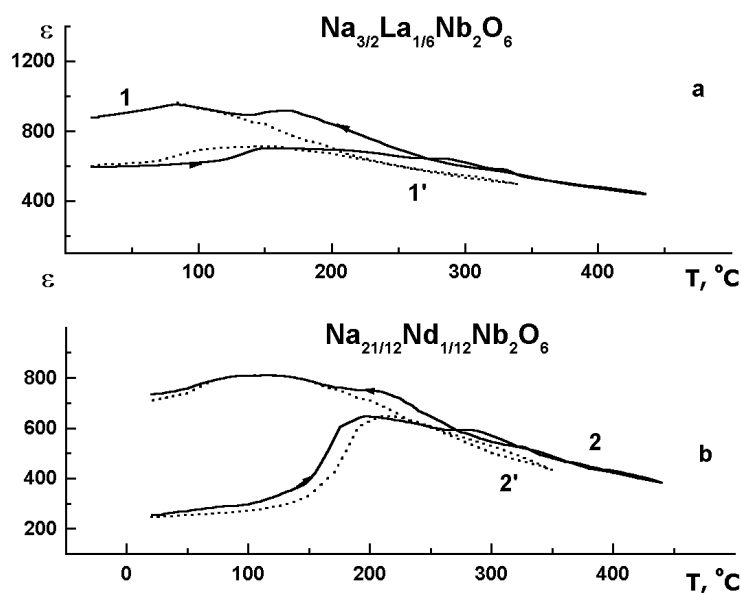


Figure 3. Temperature dependencies of the permittivity of the materials $(1 - 3x/2)\text{Ln}_{2/3}\text{Nb}_2\text{O}_6 - 3x\text{NaNbO}_3$ (1, 1' – Ln = La, $x = 1/2$; 2, 2' – Ln = Nd, $x = 7/12$) measured at 10^6 Hz (1, 2) and 10^9 Hz (1', 2') – dot line.

content. It is interesting to note that unlike pure sodium niobate NaNbO_3 , temperature dependence of the permittivity of these materials is characterized by both noticeable hysteresis and by high residual polarization which occur after heating a ceramic sample above the phase transition temperature (figure 3). The data in the figure 3 have been obtained under conditions of slow heating and cooling rates ($2\text{ }^\circ\text{C}/\text{min}$). After heating above the temperature of the phase transition, followed by slow cooling to room temperature, the permittivity magnitude increased by 200 to 500, and regressed for 50–60 hours. It should be noted that this behavior of the permittivity remains unchanged up to the frequency of 10^9 Hz which denotes that the observed behavior of the permittivity is not related to any effects of processing.

3.2. System $\text{Ba}_{6-x}\text{Ln}_{8+2x/3}\text{Ti}_{18}\text{O}_{54}$ ($\text{Ln} = \text{La, Nd, Sm}$)

The materials of the system $\text{Ba}_{6-x}\text{Ln}_{8+2x/3}\text{Ti}_{18}\text{O}_{54}$ ($\text{Ln} = \text{La, Nd, Sm}$) have got a high permittivity from 70 up to 100 which slightly decreases with the diminishing ionic size of the rare-earth element. Within the solid solubility range of $\text{Ba}_{6-x}\text{Ln}_{8+2x/3}\text{Ti}_{18}\text{O}_{54}$, the diffuse maxima of $\epsilon(T)$ and the corresponding maxima of $\tan\delta(T)$ have been revealed for different rare-earth elements containing the analogues corresponding to various x values (figure 4). At fixed ratio of composing oxides (fixed x), the anomalies revealed a shift towards high temperatures when the ionic radii of the rare-earth element decrease (figure 4). On the other hand, for a certain rare-earth element (La, Nd, or Sm) the anomaly regions shift towards high temperatures when the content of rare-earth ions decrease (i.e. increase in x) (figure 5). It should be noted that similar behavior is observed in solid solutions with

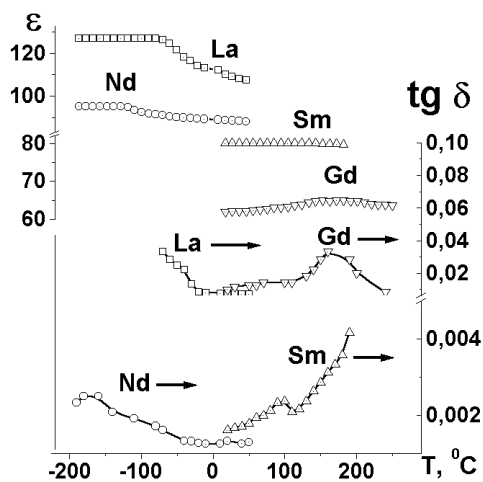


Figure 4. Temperature dependencies of the permittivity and dielectric loss tangent of the materials $\text{Ba}_{6-x}\text{Ln}_{8+2x/3}\text{Ti}_{18}\text{O}_{54}$ ($\text{Ln} = \text{La, Nd, Sm, Gd}$) measured at 10^{10} Hz .

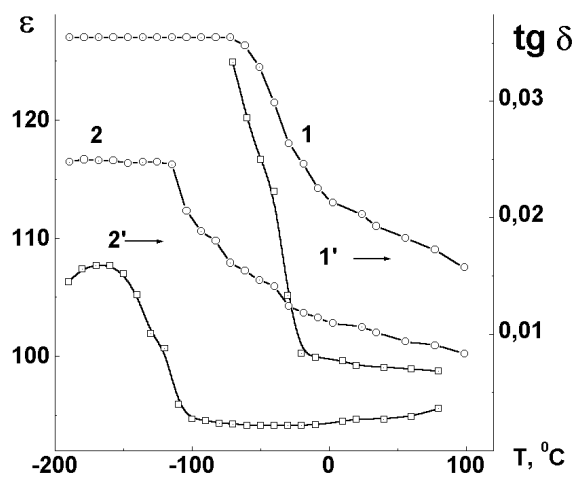


Figure 5. Temperature dependencies of the permittivity (1, 2) and dielectric loss tangent (1', 2') of the materials $\text{Ba}_{6-x}\text{La}_{8+2x/3}\text{Ti}_{18}\text{O}_{54}$ (1, 1' - $x = 1.5$; 2, 2' - $x = 2.0$) measured at 10^{10} Hz .

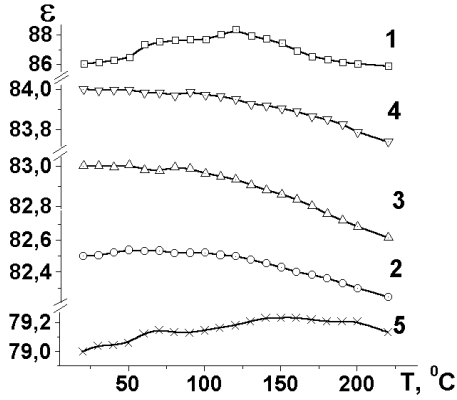


Figure 6. Temperature dependencies of dielectric permittivity in the materials $(\text{Ba}_{1-y}\text{Ca}_y)_5\text{Sm}_{8.3(3)}\text{Ti}_{18}\text{O}_{54}$ ($x = 1.0$) measured at 10^{10} Hz; $y = 0$ (1); 0.13 (2); 0.18 (3); 0.25 (4); 0.30 (5).

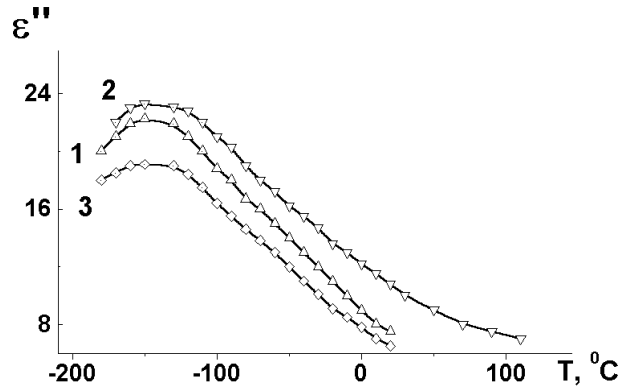


Figure 7. Temperature dependencies of the imaginary component of permittivity (ϵ'') at 96.7 GHz (1), 134 GHz (2) in the materials $\text{Ba}_{4.5}\text{La}_9\text{Ti}_{18}\text{O}_{54}$ ($x = 1.5$) and $\text{Ba}_{0.8}\text{Sr}_{0.2}\text{La}_2\text{Ti}_4\text{O}_{12}$ (3).

ferroelectric and antiferroelectric properties. However, in the case of BLTs, the hysteresis loop is not detected, and Curie-Weiss behavior is not observed in the vicinity of the anomalies. Again, partial isovalent substitution of the A-site ions results in the shift of the anomalies of $\epsilon(T)$ and $\tan \delta(T)$ towards low temperatures with the increasing content of substituting ion (Ca^{2+}) (figure 6) which is accompanied by a change in the sign of τ_ϵ around room temperature.

The measurements in the submillimeter (SMM) wavelength range revealed diffuse maxima in the temperature dependencies of both the absorption coefficient (α) and the imaginary component of the dielectric constant (ϵ'') at exactly those temperatures where the maxima of $\epsilon(T)$ were observed at microwaves (figure 7). The results indicate the non-relaxation nature of the anomalies of the dielectric parameters, and confirm that they are not related to the effects of processing.

4. Discussion

Both of the materials investigated are characterized by common structural fragments: oxygen octahedra $[(\text{Ti},\text{Nb})\text{O}_6]$, which form an oxygen network. However, the structure $\text{Ba}_{6-x}\text{Ln}_{8+2x/3}\text{Ti}_{18}\text{O}_{54}$ contains different structural A-sites: trigonal sites (empty), tetragonal sites (shared with barium and rare-earth ions), and pentagonal sites (filled with barium ions), whereas the A-sublattice of the defect perovskite $\text{Ln}_{2/3}\text{Nb}_2\text{O}_6$ contains only tetragonal sites. Again, both of the materials studied are differed by the degree of octahedral tilting which is much higher in the tetragonal tungsten bronze $\text{Ba}_{6-x}\text{Ln}_{8+2x/3}\text{Ti}_{18}\text{O}_{54}$ [10]. Recently, the authors of reference 10 assumed the effect of anharmonicity of the lattice oscillations on temperature behavior of the permittivity in $\text{Ba}_{6-x}\text{Ln}_{8+2x/3}\text{Ti}_{18}\text{O}_{54}$ solid solutions. Moreover, they

further concluded the direct dependence of lattice anharmonism on the octahedral tilting: the smaller is the degree of tilt the higher is the lattice anharmonism [10].

Whereas the permittivity of low-loss dielectrics in the MW range is mainly determined by the contribution of elastic-strain “infrared” polarization temperature, the behavior of “infrared” permittivity could be discussed in terms of simple harmonic oscillator model which also considers the anharmonic contribution into the harmonic restoring force ($f_{Ri} = -c_i x_i$) acting on an ion shifted for a distance x_i under the applied field (E). The magnitude of the harmonic restoring force f_{Ri} is equal to the distorting force $f_{Di} = q_i E$, and, therefore, the elastic coefficient c_i can be given as $c_i = q_i E / x_i$. With the increasing temperature, the ionic interaction is reduced (x_i increases due to the increase in the unit-cell volume), which results in the lowering of c_i . The anharmonic contribution of the lattice oscillations to the restoring force f_R in the first approximation could be linearly dependent on the temperature component βT , which gives us the following equation: $f_R = -(c_{\text{sum}} + \beta T)x$ [11], where c_{sum} is the elastic coefficient characterizing the total contribution of the harmonic components. Taking into account the equality of the distorting and the restoring forces affecting the ion in the crystal lattice, $q_i E = (c_{\text{sum}} + \beta T)x_i$, the polarizability of a single ion ($\alpha_i = P_i / E_i = q_i x_i / E_i = q_i^2 / (c_{\text{sum}} + \beta T)$) is inversely proportional to the restoring force. According to the above consideration, an increase in the temperature would result in different effects: the first one is related to the lowering of c_i , which consequently leads to an increase in both polarizability α_i and permittivity (i.e., the effect of harmonic contribution), whereas the second one is related to the temperature changes in anharmonic contribution βT (i.e., the effect of anharmonic contribution). The latter one causes an increase in the restoring force f_R , and, as a consequence, both the polarizability and the permittivity decrease with the temperature in such a way that higher β values correspond to higher negative values of the temperature coefficient of permittivity τ_ϵ , where $\tau_\epsilon = (1/\epsilon)(\partial\epsilon/\partial T)$. Therefore, the $\epsilon(T)$ behavior can be interpreted as a superposition of two different, competing contributions: an increase in permittivity with temperature (harmonic contribution), and a decrease in permittivity with temperature (anharmonic contribution). The resulting effect of these two contributions in a certain temperature interval may be the reason for the anomalies observed on the dependencies of $\epsilon(T)$ in the materials studied. It should be also noted that the above simple consideration does not allow for either the cooperative interaction of different ions or for the influence of electronic polarization on the “infrared” permittivity. However, a more accurate explanation of the observed temperature behavior of permittivity may be a target of further research.

An analysis of the measured data indicates that the temperature effect of the anharmonic contribution βT is also related to the flexibility of the oxygen network. In some tilted structures (BLTs with high average ionic size of A-site ions), the increasing temperature facilitates the oxygen-network flexibility due to the increase in the unit-cell volume [10]. This decreases the β value, and consequently, decreases the slope of the curve $\epsilon(T)$. On the other hand, in highly straightened structures ($\text{Ln}_{2/3}\text{Nb}_2\text{O}_6$) the β value seems to be not temperature dependent, and the anhar-

monic component βT merely increases with the temperature. As a result, highly straightened structures are characterized by ten times higher τ_ϵ values in comparison with the tilted structures. This agrees well with the authors of reference 12 who ascribed a weak effect of the dipolar mechanism, observed in the case of a tilted structure, to the decreasing tilting amplitude. Partial isovalent substitution in the A-sublattice, which diminishes the average size of A-site ions, increases the flexibility of the oxygen network. This may result in a slight shift of the $\epsilon(T)$ anomalies towards low temperatures accompanied by degradation of $\epsilon(T)$ maxima (figure 6) which enhances the temperature coefficient τ_ϵ .

Thus, it may be concluded that temperature coefficient τ_ϵ may be controlled by varying the correlation between harmonic and anharmonic contributions into the lattice oscillations which is possible by acting on the crystal lattice of the material.

References

1. Belous A.G., Novitskaya G.N., Polianetskaya S.V. // *Izvestija Akademii Nauk, ser. Neorgan. Mater.*, 1987, vol. 8, No. 23, p. 1330–1332.
2. Belous A.G., Novitskaya G.N., Polianetskaya S.V., Gornikov Y.I. // *Zhurn. Neorg. Khimii*, 1987, vol. 2, No. 32, p. 283–286 (in Russian).
3. Sych A., Demyanenko V., Nekrasov M., Zastavker L., Eremenko L. // *Inorg. Mat.*, 1973, vol. IX, No. 11. p. 1947–1950.
4. Sych A., Eremenko L., Zastavker L., Nekrasov M. // *Inorg. Mat.*, 1974, vol. X, No. 3, p. 496–500.
5. Pivovarova A., Strahov V., Melnikova O. // *Inorg. Mat.*, 1999, vol. 35, No. 9. p. 1118.
6. Masuno K. // *J. Phys. Soc. Japan*, 1964, vol. 19, No. 3, p. 323–328.
7. Negas T., Davies P.K. // *Materials and Processes for Wireless Communications, Ceram. Trans.*, 1995, vol. 53, p. 179–19.
8. Ohsato H., Mizuta M., Ikoma T., Onogi Z., Nishigaki S., Okuda T. // *J. Ceram. Soc. Japan*, 1998, vol. 106, No. 2, p. 178–182.
9. Belous A., Ovchar O., Valant M., Suvorov D. // *Appl. Phys. Letters*, 2000, vol. 77, No. 11, p. 1707–1709.
10. Valant M., Suvorov D., Rawn C.J. // *Jpn. J. Appl. Phys.*, 1995, vol. 38, No. 5A, p. 2820.
11. Poplavko Y.M. *Physics of Dielectrics*. Kiev, Vyshcha Shkola, 1980 (in Russian).
12. Colla E.L., Reaney I.M., Setter N. // *J. Appl. Phys.*, 1993, vol. 74, p. 3414.

Температурна поведінка діелектричної проникності в складних оксидах рідкісноземельних елементів зі структурою типу перовскиту

А.Г.Білоус, О.В.Овчар, Д.О.Міщук

Інститут загальної та неорганічної хімії ім. В.І.Вернадського
03680 Київ-142, просп. Палладіна, 32/34

Отримано 4 вересня 2002 р.

Керамічні матеріали на основі оксидів зі структурою перовскиту ($\text{Ln}_{2/3}\text{Nb}_2\text{O}_6$) та тетрагональної вольфрамів бронзи ($\text{Ba}_{6-x}\text{Ln}_{8+2x/3}\text{Ti}_{18}\text{O}_{54}$) досліджувались в широкому частотному та діапазонах. Встановлено присутність температурних аномалій діелектричних параметрів (ϵ , $\tan \delta$). Виявлені аномалії не пов'язані з технологічними особливостями та присутністю фазових переходів. Поведінка діелектричної проникності розглянута з позиції механізму поляризації, зв'язаного з пружно-деформаційними коливаннями кристалічної ґратки, і пояснюються взаємокомпенсуючим впливом гармонічних і ангармонічних вкладів у коливання кристалічної ґратки.

Ключові слова: діелектрична проникність, діелектричні втрати, НВЧ діелектрики

PACS: 77.22.-d, 77.22.Ch

